Quantifying the Solute Drag Effect on Ferrite Growth in Fe-C-X Alloys Using Controlled Decarburization Experiments

C. QIU, H.S. ZUROB, D. PANAHI, Y.J.M. BRECHET, G.R. PURDY, and C.R. HUTCHINSON

The kinetics of ferrite growth in the Fe-C-Co and Fe-C-Si systems has been quantified using controlled decarburization experiments. The Fe-C-Co system is a particularly interesting system since a large range of Co contents can be considered providing a suitable data set for examination of the composition dependence of the solute drag effect. Six Fe-C-Co alloys containing Co from 0.5 to 20 pct have been considered. Three Fe-C-Si alloys have also been considered and each has been transformed at three temperatures proving a suitable data set for examining the temperature dependence of the solute drag effect. This data set, along with ferrite growth data from decarburization experiments on an Fe-C-2Cr alloy has been used to test the ferrite growth model proposed in the companion article by Zurob et al. It is shown that this model for ferrite growth, that includes diffusional dissipation due to interaction between the solute and the migrating boundary, quantitatively captures both the temperature and composition dependence of the deviation of experimental ferrite growth kinetics from the PE and/or LENP models.

DOI: 10.1007/s11661-012-1547-0

I. INTRODUCTION

IT is well known that segregated impurity atoms can drastically reduce the mobility of grain boundaries in pure metals. Lucke and Detert[1] developed the first quantitative treatment of this effect to explain their observations that the recrystallization rate of high purity Al could be reduced by many orders of magnitude by the addition of 0.01 pct Mn or Fe. They attributed the effect to an interaction between the solute atoms in solution and the moving grain boundaries. The phenomenon is now considered to be a general effect and is usually referred to as the 'solute-drag effect'.

The solute-drag effect has received considerable attention both because of its scientific interest and because of the central role of interface motion during the thermomechanical processing of many industrially important alloys. Soon after the initial treatment of Lucke and Detert, Cahn[2] presented his theoretical treatment, which was later followed by similar approaches by Lucke and Stuwe[3,4] and this 'force' approach has become one of two solute drag theories that have come to dominate the physical metallurgy literature. The force approach invokes an interaction energy profile, $E(x)$, between a solute atom and a grain boundary and by solving the diffusion equation for the solute across the migrating boundary the solute concentration profile across the boundary as a function of boundary velocity can be found. The behavior of the solute under the extremes of grain boundary motion is self-evident. When the grain boundary moves with a velocity that is very slow compared to the diffusion of the solute in the vicinity of the grain boundary, the concentration profile will be close to the equilibrium profile for a stationary boundary, $C(x) = C_o \exp\left[-\frac{E(x)}{kT}\right]$, where C_o is the bulk solute content. If the grain boundary velocity is fast compared to the diffusion of the solute, then the concentration profile approaches the uniform bulk alloy composition C_o, through the boundary. However, at intermediate velocities, more interesting, asymmetric concentration profiles are possible. It should be emphasised that to calculate such profiles it is necessary to quantitatively describe the solute interaction profile with the boundary, $E(x)$, and the solute diffusivity across the boundary, $D(x)$, neither of which is known with much certainty.

Cahn argued that an impurity atom will be attracted to the centre of the boundary with a force, $^{dE}/_{dx}$. The solute atom exerts an equal and opposite force on the boundary and the net force can be found by summing the forces from each of the atoms over the entire boundary. For a stationary boundary with the symmetric equilibrium solute concentration profile the net force sums to zero. For asymmetric profiles a net drag force results. Cahn summed the forces to obtain a net 'solute drag' force, P, on the boundary:

$$P = -\int_{-\infty}^{+\infty} \frac{(C - C_o)}{V_m} \frac{dE}{dx} dx \qquad [1]$$

where V_m is the molar volume and C_o is the bulk solute content.

CONG QIU, Ph.D. Student and CHRISTOPHER HUTCHINSON, Associate Professor and ARC Future Fellow, are with the Department of Materials Engineering, Monash University, Clayton, VIC 3800, Australia. Contact e-mail: christopher.hutchinson@monash.edu HATEM ZUROB, Associate Professor, GARY PURDY, Professor, and DAMON PANAHI, Ph.D. Student, are with the Department of Materials Science and Engineering, McMaster University, Hamilton, ON, Canada, YVES BRECHET, Professor, is with the SIMAP, Institut National Polytechnique de Grenoble, 38402 St Martin D'Hères, France.
Manuscript submitted June 30, 2012.
Article published online December 11, 2012

The drag effect increases with increasing solute content and decreasing temperature. There have been few attempts to quantitatively test the Cahn–Lucke–Stuwe theory. Part of the problem lies in the lack of knowledge regarding the best choices of $E(x)$ and $D(x)$ and that the theory should be tested as function of boundary velocity, temperature and solute content. Sinclair *et al.*[5] have performed such experiments in the Fe-Nb binary system by studying recrystallization and grain growth in an Fe/Fe-Nb diffusion couple transformed within a temperature gradient. The evolution of the microstructure was satisfactorily described using the Cahn–Lucke–Stuwe solute drag theory with appropriate choices of $E(x)$ and $D(x)$.

The second popular 'solute-drag' theory is due to Hillert[6,7] and his 'dissipation' approach was applied to both grain and phase boundaries. Hillert views the retarding effect of the solute on the moving boundary as work done by the boundary and this work may be expressed as a dissipation of Gibbs free energy (ΔG^{diss}) due to the irreversible nature of the diffusion of solute across the migrating boundary. Hillert summed the dissipation of Gibbs energy as:

$$\Delta G^{diss} = PV_m = -\int_{-\infty}^{+\infty} (C - C_o)\frac{d\mu}{dx}dx \qquad [2]$$

where μ is the chemical potential.

For a stationary grain boundary with the equilibrium concentration profile, there is no force acting on the solute atoms since no gradients in chemical potential exist at equilibrium. According to Hillert's dissipation approach, a contribution to the retarding effect of the solute arises whenever there is diffusion in response to a deviation of the concentration from the equilibrium value. For grain boundaries, Cahn's 'force' approach and Hillert's 'dissipation' approach give identical results.[8] However, for phase transformations, Hillert's dissipation approach suggests that a retarding effect of solute on the migrating boundary can exist even if there is no interaction of the solute with the migrating boundary. Such a contribution arises from the diffusion of solute across the migrating boundary driven by chemical potential differences between the product and parent phases (*i.e.* any phase transformation accompanied by a change in chemistry could exert such an effect). Over the years, a number of authors have attempted to extend the Cahn–Lucke–Stuwe 'force approach' to phase transformation, *e.g.*, References 9–11 with various degrees of success. It should be emphasized that Cahn, Lucke and Stuwe never applied or recommended applying their expression, derived for grain boundaries, to phase transformations.

These effects have received considerable attention from the community interested in describing the kinetics of ferrite formation from austenite in Fe-C-X steels and a number of attempts to interpret the results or to apply various formulations of 'solute drag' or 'dissipation due to diffusion in the interface' to migrating phase boundaries have been performed, *e.g.* References 9,10,12–17. The topic remains of interest because the existing formulations do not generally provide satisfactory agreement between experimental observations and model predictions. In the companion paper by Zurob *et al.*,[18] a model for ferrite growth is proposed that incorporates Hillert's dissipation approach to quantify the effect of substitutional solute additions (X) on migrating ferrite/austenite phase boundaries in Fe-C-X systems. Zurob *et al.* considered two extreme cases in their discussion—the Fe-C-Mo and the Fe-C-Ni/Mn systems. Under the conditions considered, there is no chemical potential gradient for Mo between the ferrite and austenite of bulk composition in the Fe-C-Mo system. As such, the phase interface in the Fe-C-Mo system is a pseudo grain boundary from the point of view of the Mo (Figure 1(b)). The Mo solute was assumed to interact strongly with the migrating phase boundary. In this case the 'dissipation' is due entirely to the diffusion of Mo in the vicinity of the interface due to its preferred interaction with the boundary.

In the Fe-C-Ni and Fe-C-Mn systems, there exists a chemical potential gradient for Ni or Mn between the ferrite and austenite, and consequently there is a driving force for alloying element transfer from the ferrite to the austenite. It was assumed that the alloying element did not interact strongly with the boundary itself, which based on experimental studies seems a reasonable assumption (Figure 1(c)). In this case, the dissipation due to the alloying element is due to the diffusion from the ferrite to the austenite across the boundary in response to the driving force for bulk solute partitioning.

Other alloy systems lie between the two extremes discussed by Zurob *et al.*[18] and hence contributions to

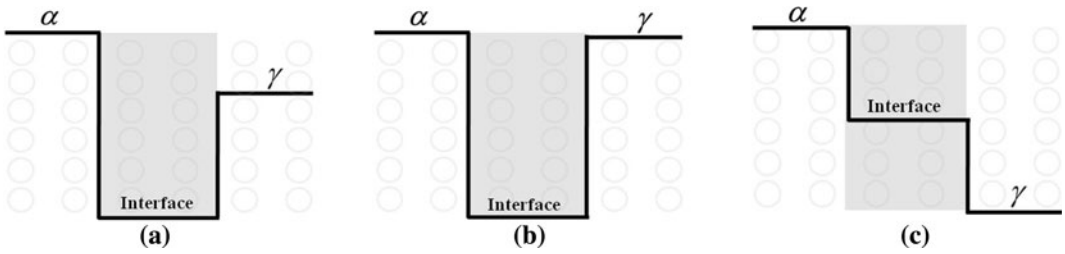

Fig. 1—Schematic representations of the interaction profiles between solute atoms and phase boundaries: (*a*) the general case where an interaction between the interface and the solute exists as well as a bulk partitioning tendency for the solute, (*b*) the case where an interaction with the boundary exists but there is no bulk partitioning tendency, Fe-Mo is an example of such behavior, (*c*) the case where the interaction of the solute with the boundary is weak but there exists a bulk partitioning tendency for the solute, Fe-Ni and Fe-Mn are examples of such behavior.

the dissipation due to solute diffusion may arise from both the interaction with the boundary and due to diffusion across the boundary driven by solute partitioning tendencies between the bulk phases (Figure 1(a)). It may be reasonable to extrapolate expectations of the solute concentration, temperature and interface velocity dependence of the dissipation from grain boundaries for the dissipation arising from the solute interaction with the phase boundary (*e.g.* Fe-Mo, Figure 1(b)), but the situation is much less clear for the general phase transformation where a dissipation due to cross-boundary diffusion in response to bulk partitioning tendencies may exist. Depending on the temperature dependence of the partitioning behavior of the solute it is conceivable that situations may exist where the overall solute drag effect even increases with increasing temperature, *i.e.* the opposite dependency that would be predicted by extrapolating from grain boundaries.

It is this question that provides the motivation for this study. In order to quantitatively test the ferrite growth model proposed by Zurob *et al.*[18] it is necessary to test, as a function of solute concentration, temperature and interface velocity, the kinetics of phase transformations in systems where dissipations due to solute interactions with the boundary and due to diffusion in response to chemical potential gradients between the bulk phases exist.

To make this comparison between model and experiment, high precision ferrite growth data is required as a function of both temperature and bulk solute content. Decarburization experiments, where ferrite grows in from the surface of a sample in a highly planar manner, has been shown to be a useful approach to obtain measurements of ferrite growth with high precision[19–23] (errors of $\pm$ 5 μm on ferrite layer thicknesses from 50 to 500 μm). This is the approach adopted in this study.

II. EXPERIMENTAL PROCEDURE

Ferrite growth from austenite has been studied in this work using decarburization. Three alloy systems (Fe-C-Co, Fe-C-Si and Fe-C-Cr) have been selected to monitor the ferrite growth kinetics as both a function of temperature and bulk solute content. The data for Fe-C-Cr is taken from a recent publication[21] and new alloys from the Fe-C-Co and Fe-C-Si systems have been prepared for this study. Both Si and Co are ferrite stabilizers and hence during growth there is a driving force for partitioning of Si and Co from the austenite to the ferrite. The alloy compositions prepared are listed in Table 1.

The Fe-C-Co system is a particularly interesting system to use for a test of the composition dependence of the solute drag effect on ferrite growth because the thermodynamics allow a large range of solute contents to be examined by decarburization. Solute contents up to 20Co (wt pct) have been prepared. Isoplethal sections for selected alloys are shown in Figure 2.

Decarburization experiments can only be performed within the temperature range above the eutectoid temperature and below the temperature where ferrite of zero C content is no longer stable. At 1098 K (825 °C), Co contents up to 20 pct can be examined and for an alloy such as that containing 5Co, decarburization experiments can be performed at temperatures ranging from 1048 K to 1173 K (775 °C to 900 °C). In this study, five Co compositions are examined at 1098 K (825 °C) and the 20Co alloy is examined at 1148 K (875 °C) (Figure 2(d)) to test the concentration dependence of the solute drag effect. The 20Co alloy was originally designed to have 1C (wt pct) which would allow this composition to be transformed at 1098 K (825 °C) however, ICP chemical analysis showed a slightly lower carbon composition and as a result the 20Co alloy is instead transformed at 1148 K (875 °C). Three temperatures are examined in the alloy containing 5Co (Figure 2(c)) [1048 K, 1098 K and 1123 K (775 °C, 825 °C and 850 °C)] to test the temperature dependence.

Three Si-containing alloys, with compositions up to 1.5Si (Table 1) are also examined and isoplethal sections for these three alloys are shown in Figure 3. In this case, each of the three Si containing alloys was transformed at a number of temperatures to monitor both the concentration and temperature dependence of the solute drag effect. The 0.45Si and 0.86Si alloys were transformed at 1048 K, 1079 K, 1098 K and 1123 K (775 °C, 806 °C, 825 °C, and 850 °C), whilst the 1.46Si alloy was transformed at 1098 K and 1123 K (825 °C and 850 °C).

The alloys were produced by arc melting from elemental materials of purity greater than 99.9 pct. The ingots weighed approximately 50 g. Each ingot was melted 6 times under an Ar atmosphere. The ingots were hot rolled to 50 pct reduction at ~1073 K (800 °C), followed by homogenization at 1423 K (1150 °C) for 4 days encapsulated in quartz.

Samples for decarburization were electroplated with a layer of pure Fe of ~5 to 10 μm thickness prior to decarburization. The electroplating was made in a distilled water based solution containing 2.3 mol/L $FeCl_2$ and 1 mol/L NaCl using a 25 to 30 mA current applied from a counter electrode (pure iron) to the working electrode (samples) for 10 minutes at 353 K to 358 K (80 °C to 85 °C). The reason for the deposition is to avoid preferential Co or Si oxidation at the surface of the material during decarburization that may influence the ease of C removal from the surface during the decarburization process. This has been observed to sometimes be a problem in alloys containing 2Si (wt pct) and this is the reason for

Table 1. Alloy Compositions Fabricated for This Study

Fe-C-Si Alloy Compositions (wt pct)	Fe-C-Co Alloy Compositions (wt pct)
Fe-0.74C-0.45Si	Fe-0.80C-0.49Co
Fe-0.76C-0.84Si	Fe-0.83C-0.98Co
Fe-0.75C-1.46Si	Fe-0.79C-1.93Co
	Fe-0.80C-4.78Co
	Fe-0.77C-10.0Co
	Fe-0.78C-20.0Co

The compositions listed were measured by ICP after homogenization of the alloys.

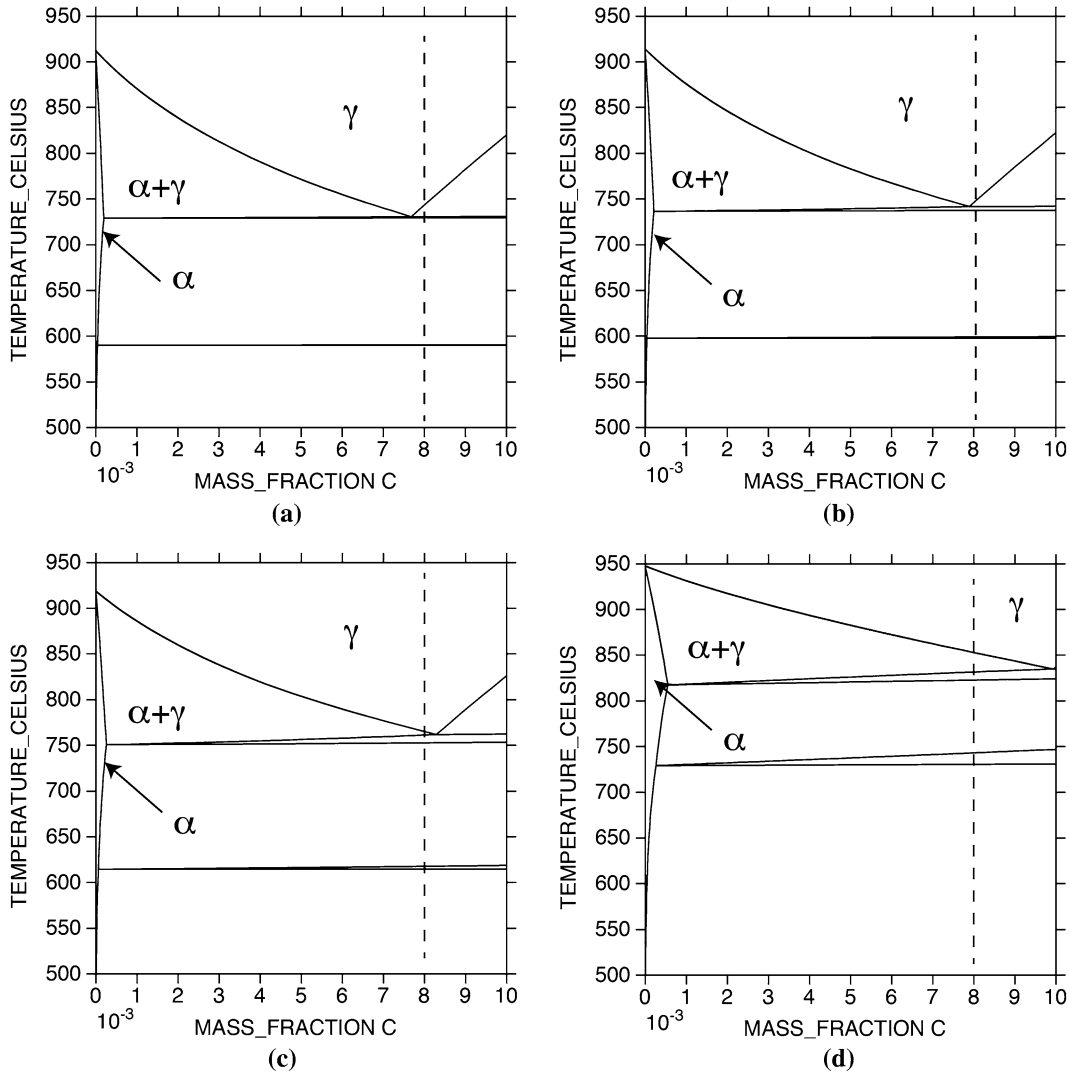

Fig. 2—Isopleth sections from the Fe-C-Co system at (*a*) 0.49Co, (*b*) 1.93Co, (*c*) 4.78Co and (*d*) 20Co (wt pct). The austenite (γ), ferrite (α) and $\gamma+\alpha$ two phase fields are indicated. The bulk C contents of the alloys are indicated by the vertical dotted line.

not extending the Si alloy series to 2Si, even though the thermodynamics would allow this.

The decarburization process was conducted in a specially designed, atmosphere controlled vertical tube furnace. The samples were brought to temperature in an Ar atmosphere and once equilibrated at temperature, pure H_2 is passed through water and through the furnace. The sample stage holds five samples that can be dropped into a quenching bucket containing water, under atmosphere, at the pre-selected aging times. The temperature is monitored by two thermocouples that are located less than 1 cm from the samples.

After decarburization, samples were sectioned, mounted, metallographically polished and etched and the ferrite growth layer was measured.

III. RESULTS

The experimentally measured ferrite layer thicknesses in the Fe-C-Co system, as a function of Co content transformed at 1098 K (825 °C) (and 1148 K (875 °C) for the 20Co alloy), and as a function of temperature in the 5Co alloy, are shown in Figures 4 and 5, respectively. In all cases, within experimental uncertainty, the growth kinetics are closely parabolic. At 1098 K (825 °C), the experimental measurements agree well with the PE or LENP model for the low Co containing alloys, but for Co contents of 5 pct or greater, the kinetics are measurably slower (*i.e.* a solute drag effect exists).

The 5Co-containing alloy was chosen to test the temperature dependence and the data shown in Figure 5 illustrates that again the experimental measurements are parabolic, within experimental error, and that the kinetics agree well with the LENP or PE model predictions at 1123 K (850 °C), but the deviation from the LENP and PE models increases with decreasing temperature. At 1048 K (775 °C) the experimental kinetics are significantly slower than the LENP or PE model predictions.

The experimental ferrite layer thicknesses, measured as a function of temperature, are shown in Figures 6 through 8, for the alloys containing 0.45Si, 0.84Si and

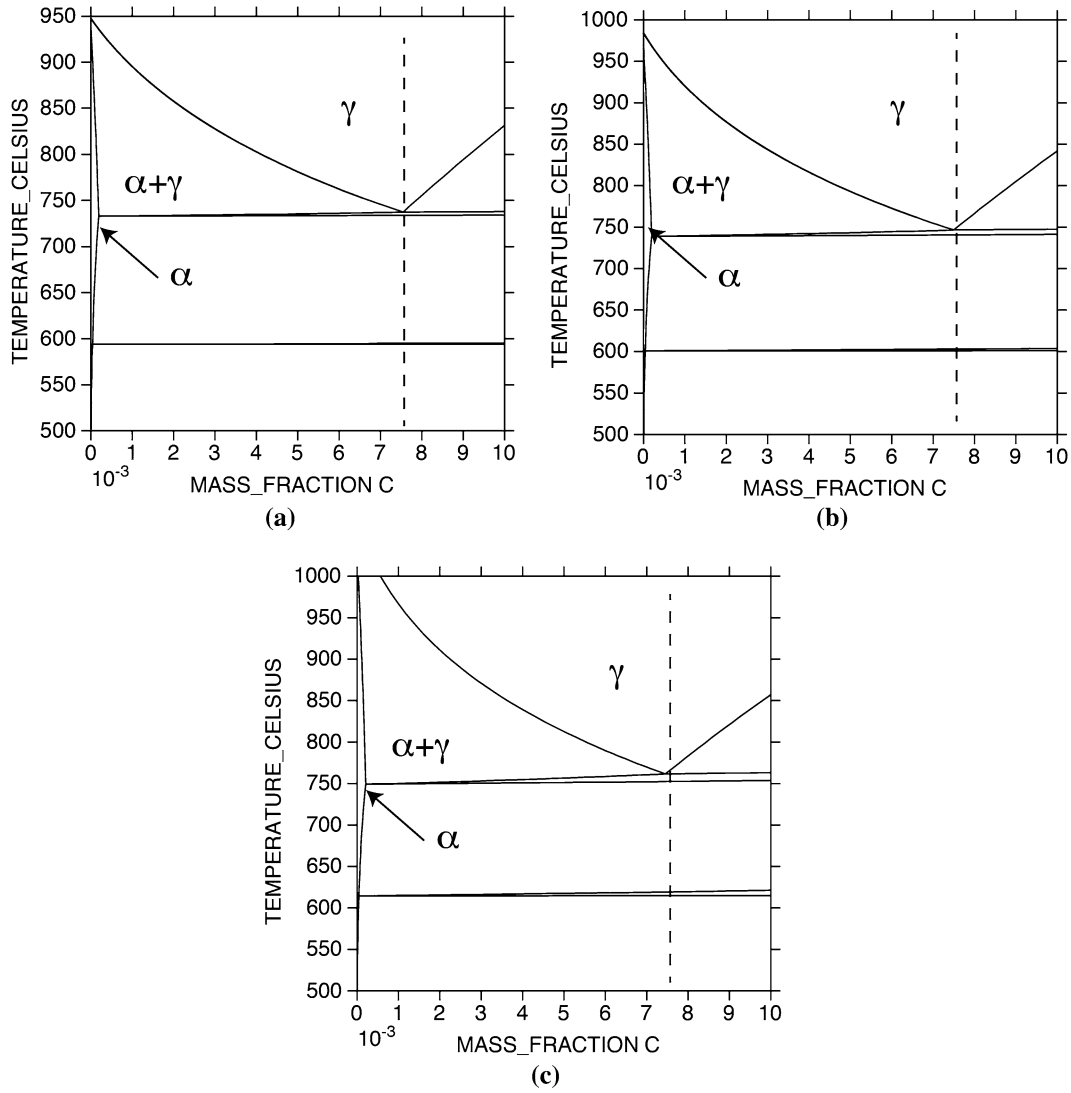

Fig. 3—Isopleth sections from the Fe-C-Si system at (*a*) 0.45Si, (*b*) 0.84Si and (*c*) 1.46Si (wt pct). The austenite (γ), ferrite (α) and $\gamma+\alpha$ two phase fields are indicated. The bulk C contents of the alloys are indicated by the vertical dotted line.

1.46Si, respectively. As was the case for the series of Co alloys examined, the growth kinetics are again closely parabolic within experimental error. The three alloys shown similar trends—at the highest temperatures the growth kinetics are close to the predictions of the LENP or PE models but as the temperature is lowered, the experimental kinetics are slowed with respect to these growth models.

The data above, for the Fe-C-Co and Fe-C-Si systems provides a suitable dataset with which the temperature and composition dependence of the ferrite growth model of Zurob *et al.* can be compared. This is the subject of Section IV.

IV. DISCUSSION

The ferrite growth data presented in Section III have been compared with the ferrite growth model of Zurob *et al.*[18] The interested reader is referred to the companion paper for the full model description but the essential characteristics of the model are summarised here.

The Zurob *et al.* model self-consistently describes the alloying element diffusion across the interface and the associated free energy dissipation, the evolution of the corresponding interfacial carbon concentration, carbon diffusion in the bulk phases and the interface velocity. The interface is treated in a discrete manner where solute atoms jump from the ferrite into the interface, jump within the interface, and jump from the interface into the austenite (Figure 9).[18]

The jumps in Figure 9 are assumed to occur with diffusion coefficients of D_1, D_2 and D_3, respectively. The evolution of the alloying element concentration on plane '*i*', dx_X^i, as a result of these jumps can be expressed as:

$$dx_X^i \cdot \frac{\delta}{V_m dt} = J_X^i - J_X^{i+1} + \frac{v}{V_m}\left(x_X^{i+1} - x_X^i\right) \quad [3]$$

where the flux term from plane '$i-1$' to plane 'i', J_X^i, is given by:

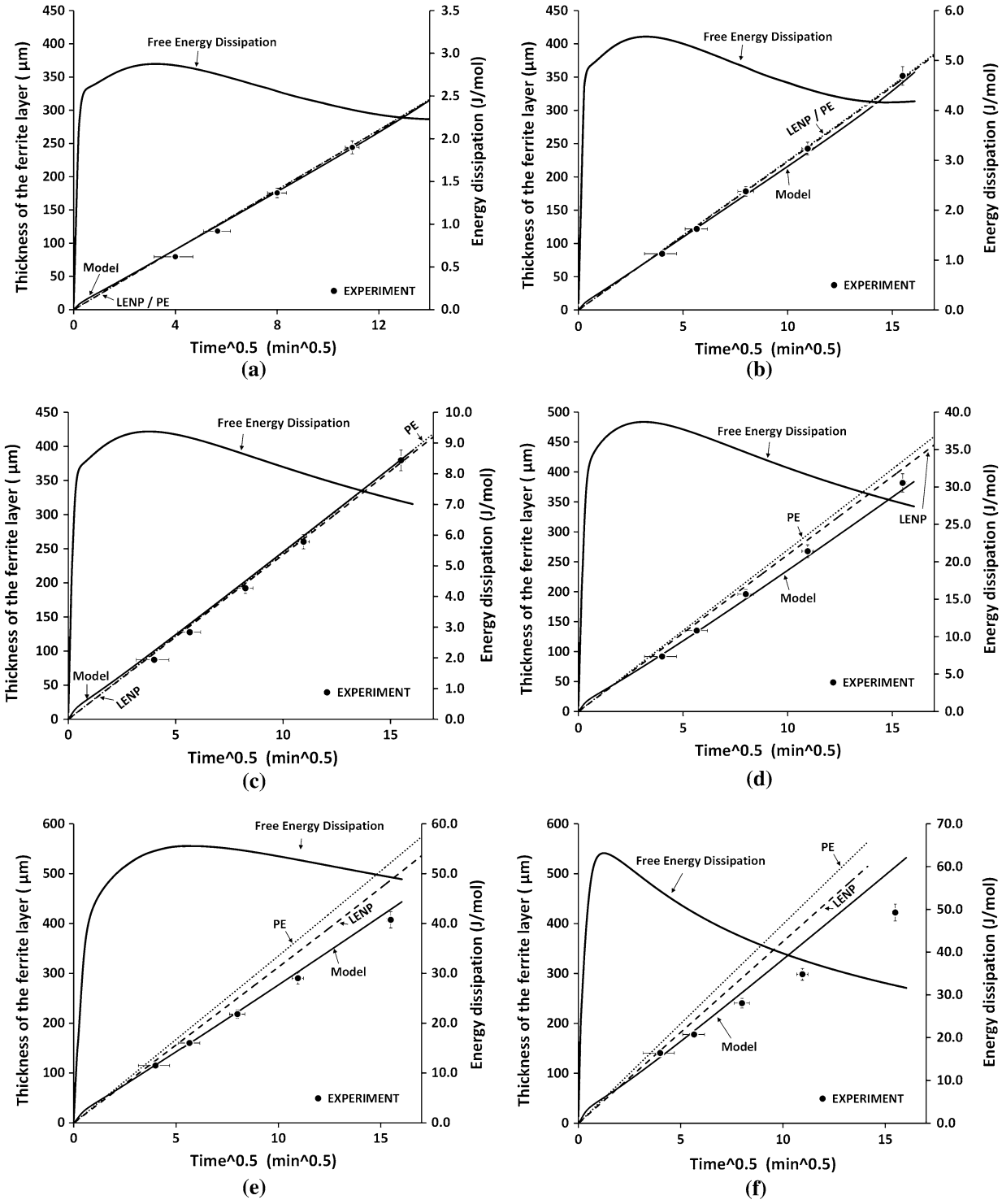

Fig. 4—Experimental ferrite layer growth kinetics measurements from the Fe-C-Co system: (*a*) Fe-0.80C-0.49Co at 825 °C, (*b*) Fe-0.83C-0.98Co at 825 °C, (*c*) Fe-0.79C-1.93Co at 825 °C, (*d*) Fe-0.80C-4.78Co at 825 °C, (*e*) Fe-0.77C-10Co at 825 °C and (*f*) Fe-0.78C-20Co at 875 °C. Comparisons with the PE, LENP and Zurob *et al.* model are shown in each case as well as the free energy dissipated during the reaction.

$$J_X^i = -\frac{D_X^i}{V_m RT} x_{\mathrm{Fe}}^{i-1} x_X^{i-1} \cdot \frac{\left(\mu_X^i - \mu_X^{i-1}\right) - \left(\mu_{\mathrm{Fe}}^i - \mu_{\mathrm{Fe}}^{i-1}\right)}{\delta} \quad [4]$$

In this equation, D_X^i are the diffusion coefficients of the substitutional element (X) as defined in Figure 9, R is the gas constant, dt is the time increment used in the calculations, δ is the distance between atomic planes, and v is the interface velocity.

A preferred interaction between the solute atoms and the interface may exist. To implement the model, choices for the interaction energy between the solute and the boundary, as well as the mass transfer coefficients (D^i)

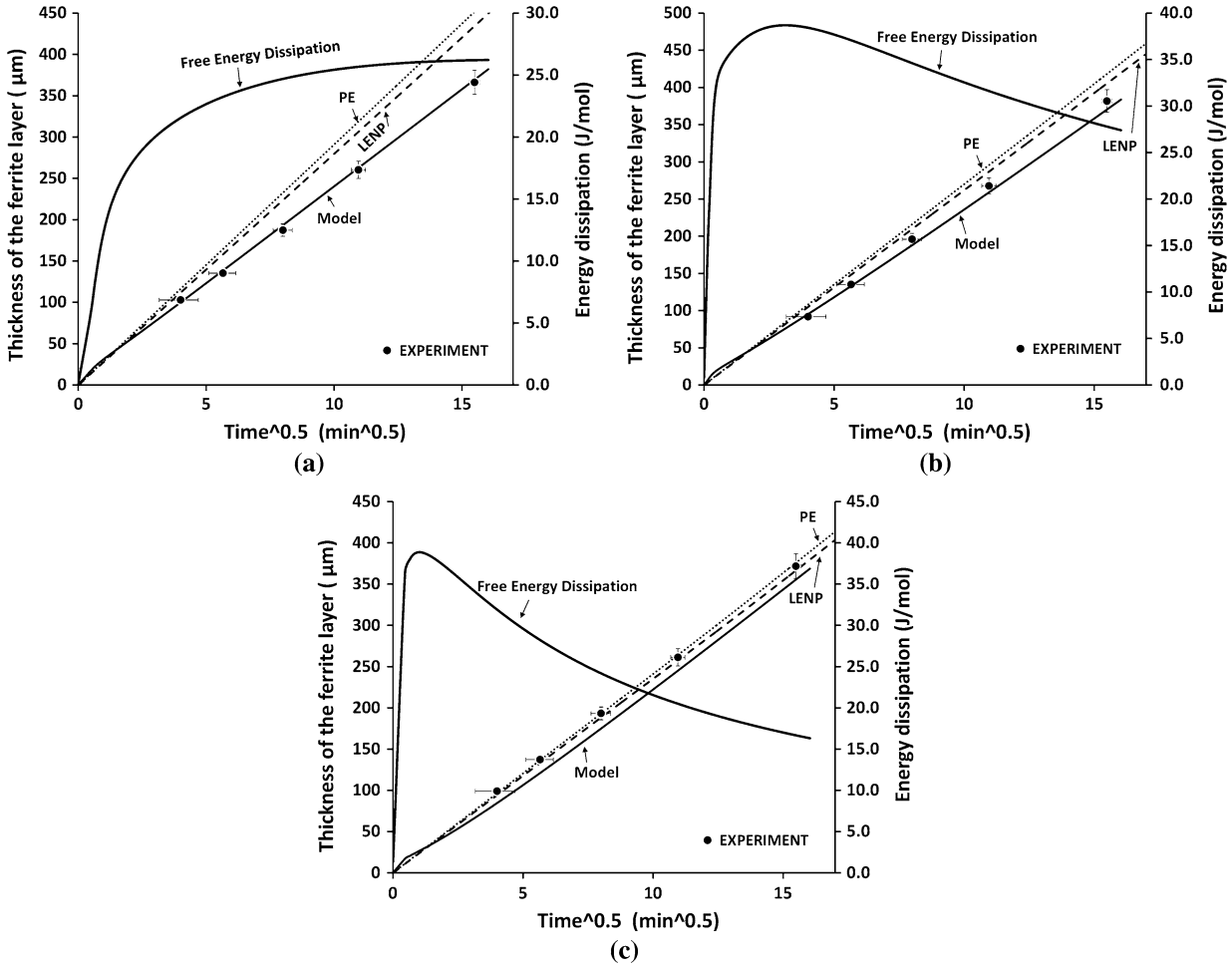

Fig. 5—Experimental ferrite layer growth kinetics measurements from the Fe-0.80C-4.78Co alloy: (*a*) 775 °C, (*b*) 825 °C, (*c*) 850 °C. Comparisons with the PE, LENP and Zurob *et al.* model are shown in each case as well as the free energy dissipated during the reaction.

controlling the jumps into and out of the interface must be made. The free energy dissipation associated with the diffusion of the substitutional alloying elements in the interface is quantified using Hillert's approach[7] (Eq. 5), and the contact conditions for the carbon at the interface in the ferrite and austenite are calculated by assuming no carbon chemical potential gradients exist over the interface and by use of a driving force equation which depends on the interfacial compositions of the substitutional alloying elements,[24] which evolve during growth.

$$\Delta G^{\text{dissipated}} = -\frac{V_m}{v}\int_{-\delta}^{+\delta} J_X \cdot \frac{d(\mu_X - \mu_{Fe})}{dy} \cdot dy \qquad [5]$$

This model has been applied to the Fe-C-Si and Fe-C-Co measurements presented in Section 3 and to the data for the Fe-C-Cr system taken from the literature.[21] Zurob *et al.* applied the model to the Fe-C-Ni, Fe-C-Mn and Fe-C-Mo systems in the companion paper.

For the Fe-C-Co system, the thermodynamic description of the interface was based on that of the FCC phase with reference states of the end components shifted 3.5 kJ/mol to simulate an interfacial energy of 0.5 J/m^2. The choice of 0.5 J/m^2 for the interphase boundary energy of a γ/α interface was set arbitrarily but acknowledging that it should lie in the range 0.1 to 1 J/m^2 for an interface between two solution phases. Since there is no well defined orientation relationship between the growing ferrite and the austenite, a value of ~0.5 J/m^2 (typical for high angle grain boundaries) seems a reasonable choice. The interaction parameter between Fe and Co in the interface was varied such that the initial chemical potential of Co in the interface is 2 kJ/mol lower than the average initial chemical potentials of Co in ferrite and austenite. As for diffusion across the interface, the effective diffusivity for the jumps from the ferrite into the interface (D1) was equated to the diffusion coefficient in bulk ferrite, the diffusivity of the jumps within the interface (D2) was equated to the geometric average of the diffusion coefficients in ferrite and austenite and the diffusivity controlling the jumps from the interface into the

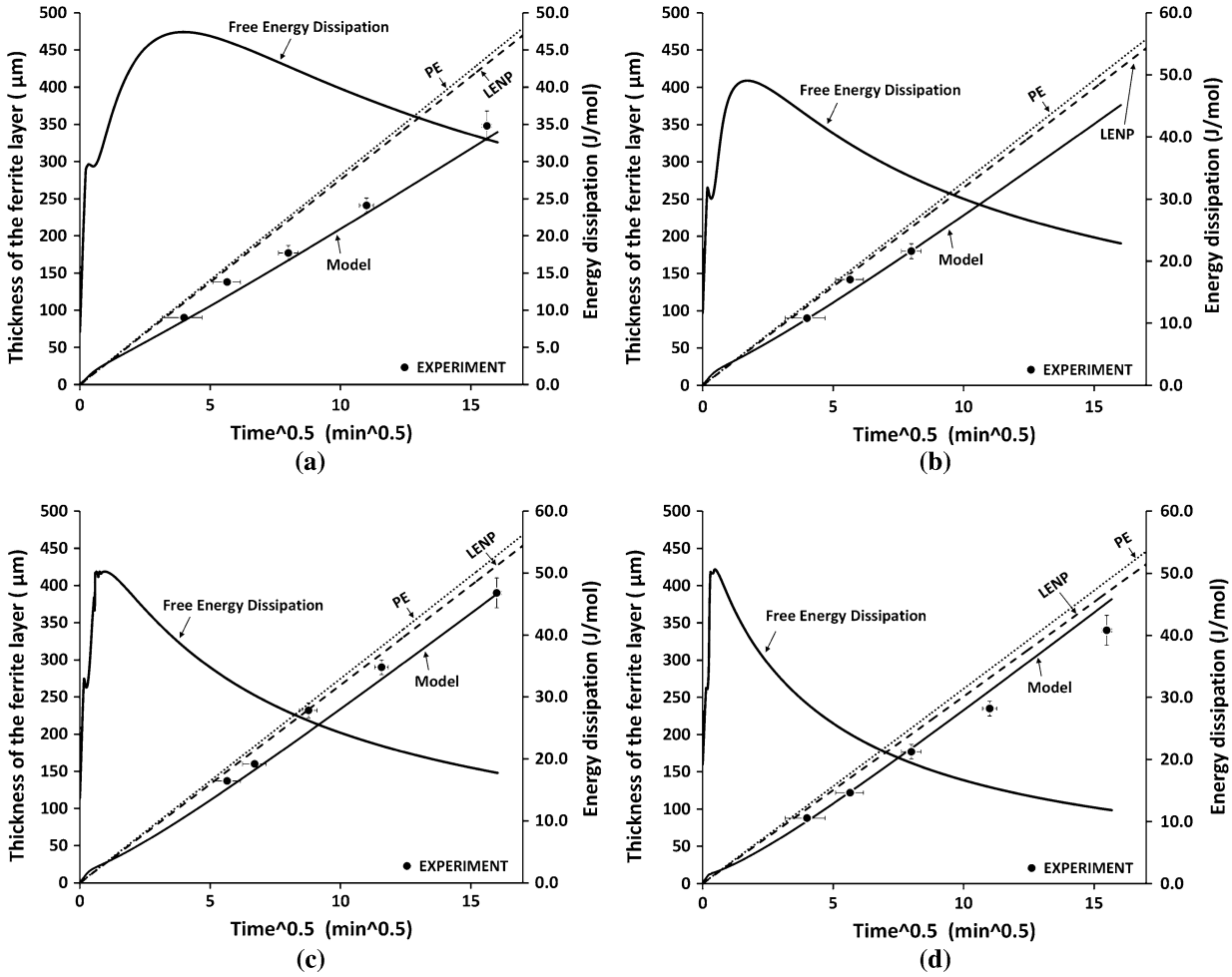

Fig. 6—Experimental ferrite layer growth kinetics measurements from the Fe-0.74C-0.45Si alloy: (*a*) 775 °C, (*b*) 806 °C, (*c*) 825 °C, (*d*) 850 °C. Comparisons with the PE, LENP and Zurob *et al*. model are shown in each case as well as the free energy dissipated during the reaction.

austenite (D3) was taken as the bulk diffusion coefficient in austenite.

The predictions of the model using this set of parameters, as a function of both Co concentration and temperature are compared with the experimental measurements in Figures 4 and 5. In all cases except the 20Co alloy, excellent agreement between the model and the experiments is achieved—both the solute dependence and the temperature dependence are well captured by the ferrite growth model. In the case of the 20Co alloy, the experimental kinetics are slower than the model predictions. The TCFe database available from Thermocalc was used for the thermodynamic calculations and their recommendation is that this is applicable for Co contents up to 20 (wt pct). As a result, the highest Co containing alloy is at the limit of the suggested valid range for the thermodynamic descriptions of the ferrite and austenite and this should be kept in mind when considering the comparison between calculation and experiment. High Fe-Co alloys are also known to show the invar effect which may affect the accommodation of elastic and plastic strains, although the present authors doubt that this is an important effect at the high temperatures considered in this study. The dissipation of free energy associated with the diffusion of the substitutional elements across the interface is also shown for each condition examined. There are two characteristics worth emphasizing: under conditions where the experimental measurements agree well with the LENP or PE models, the dissipations are small (<10 J/mol), and for conditions where a significant deviation from the LENP or PE model is observed, the dissipation passes through a maximum at short times (<2 min) and after that vary only slowly. It is this slow variation of the dissipation that accounts for the closely parabolic nature of the experimental ferrite growth kinetics. It is particularly pleasing that the model, using a single set of self-consistent parameters, is able to capture quantitatively both the transition from significant to negligible solute drag effect with decreasing solute content or increasing temperature.

The model has also been applied to the Fe-C-Si system. The Gibbs energy of the interface was derived using the same approach used for the Fe-Co-C system—the thermodynamic description of the interface was based on that of the FCC phase with reference states of the end components shifted to simulate an interfacial energy of 0.5 J/m^2. The Fe/Si interaction

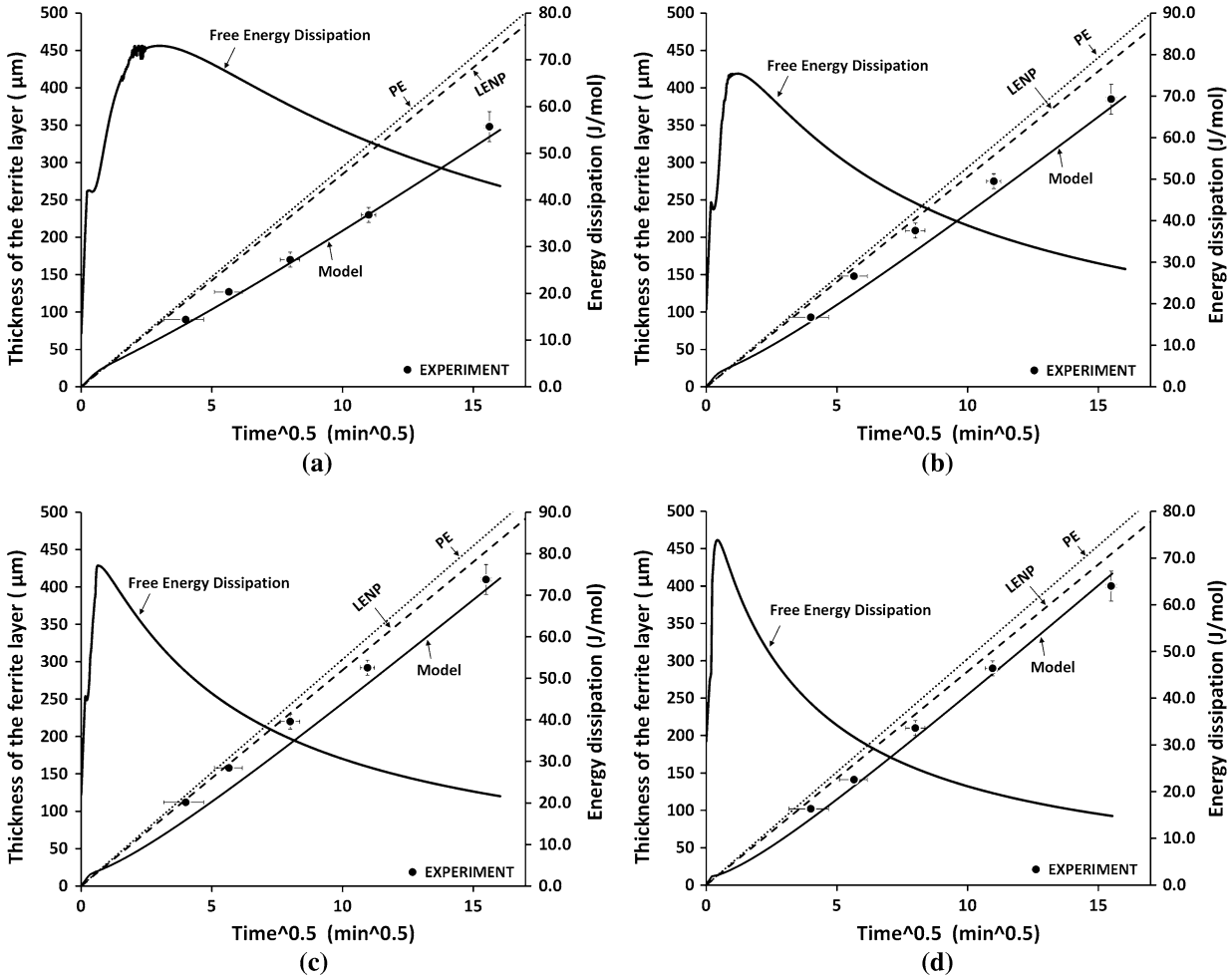

Fig. 7—Experimental ferrite layer growth kinetics measurements from the Fe-0.76C-0.84Si alloy: (*a*) 775 °C, (*b*) 806 °C, (*c*) 825 °C, (*d*) 850 °C Comparisons with the PE, LENP and Zurob *et al*. model are shown in each case as well as the free energy dissipated during the reaction.

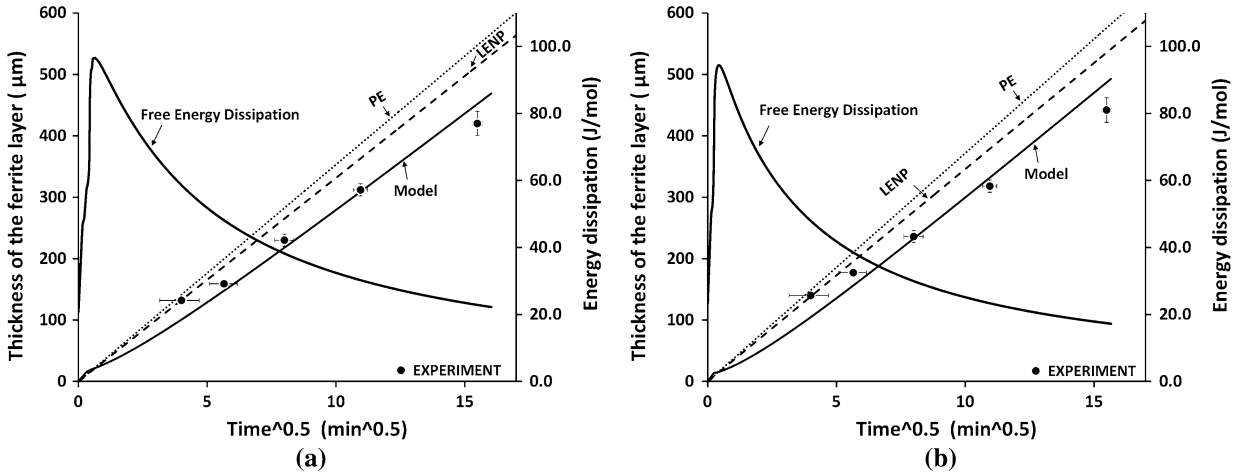

Fig. 8—Experimental ferrite layer growth kinetics measurements from the Fe-0.75C-1.46Si alloy: (*a*) 825 °C, (*b*) 850 °C. Comparisons with the PE, LENP and Zurob *et al*. model are shown in each case as well as the free energy dissipated during the reaction.

parameter in the interface was varied such that initially the chemical potential of Si in the interface is 9 kJ/mol lower than the average of the chemical potentials of Si in ferrite and austenite. Best match of the experimental observation was obtained by setting D1 equal to the diffusion coefficient in the bulk ferrite and equating D2

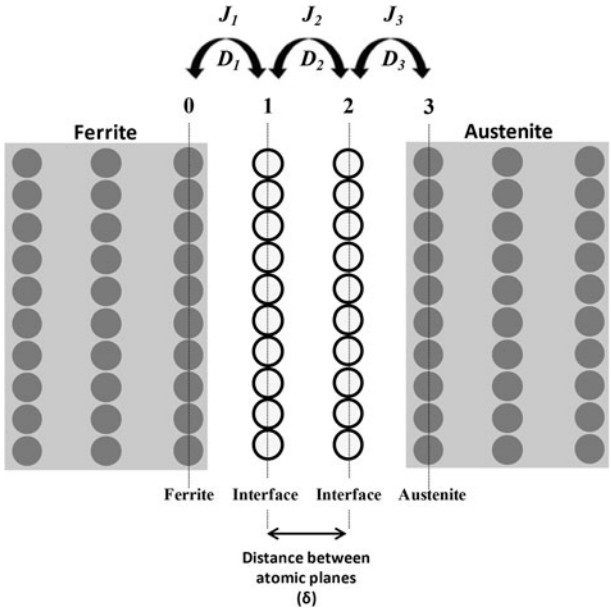

Fig. 9—Interface model in terms of atomic planes (0,1,2,3) and definition of the various diffusivities (D_1, D_2, D_3), jumps and fluxes (J_1, J_2, J_3).

and D3 to the bulk diffusion coefficient in austenite. It should be noted that in the case of the Fe-C-Co alloys, D2 was the geometric mean of the diffusivity in the ferrite and austenite but in the case of the Fe-C-Si alloys, a value equal to the diffusivity in austenite provided the best fit to experiments. It is clear that further work to understand the most appropriate choices of trans-interface diffusivities is required.

As was the case for the Co containing alloys, very good agreement is observed between model and experiment for each of the three Si containing alloys, as a function of temperature. The dissipations pass through a maximum at short times, as was the case for the Co containing alloys, but the magnitude of the dissipations is significantly larger, in some cases coming close to 100 J/mol (Fig. 8). It is particularly interesting to see that the dissipation does evolve significantly during growth. For example, the dissipation in the 1.46Si containing alloy at 1098 K (825 °C) varies by 40 J/mol between the times of the first and final data point. 40 J/mol is greater than the maximum dissipation observed in all of the Co containing alloys except that containing 20Co. Despite this significant time evolution of the dissipation in the Si containing systems, the predicted kinetics are relatively parabolic and agree well with the experimental measurements. This highlights an important point that a certain quantity of additional dissipation does not necessarily manifest itself in the same way for all Fe-C-X systems—in some systems a large deviation from LENP or PE may result and in others, almost no effect might be observed. The effect depends on the shapes of the free energy curves of the ferrite and austenite. Nevertheless, the agreement as both a function of Si content and temperature, between experiment and the Zurob *et al.* model is encouraging.

Experimental results were obtained for some of the Fe-Si-C alloys at 1173 K (900° C). The calculated dissipation at this temperature was too large compared to the driving force and solutions could not be found using the values of the interaction parameter reported earlier. If the tendency for Si segregation to the interface is reduced ($\Delta\mu = -5$kJ/mol instead of -9kJ/mol), the above problem is avoided, but the resulting kinetics are significantly faster than the experimental observations. In addition to these difficulties, the application of the model at this temperature is questionable because the high diffusion coefficient of Si in austenite would result in a spike of ~5 atomic layers. In its present form, the model does not consider bulk alloying element diffusion in austenite and is therefore not suitable for modelling the results at 1173 K (900 °C).

Application of the model to the decarburization kinetics of an Fe-0.58C to 1.99Cr (wt pct) alloy reported by Beche *et al.*,[21] as a function of temperature [1123 K, 1098 K, 1079 K, and 1048 K (850 °C, 825 °C, 806 °C, and 775°C)] is shown in Figure 10. Again, the thermodynamic description of the interface was based on that of the FCC phase with reference states of the end components shifted to simulate an interfacial energy of 0.5 J/m^2 and the interaction parameter between Cr and Fe in the interface was varied to produce an initial chemical potential in the interface which is 1.5 kJ/mol lower than the average of the initial chemical potentials of Cr in ferrite and austenite. The diffusion coefficients used, were the bulk diffusion coefficient in ferrite for D1, the geometric average of the bulk diffusion coefficients in ferrite and austenite for D2 and the bulk austenite diffusion coefficient for D3.

The agreement between model and experiment is again good and the transition from negligible additional dissipation at 1123 K (850 °C) to a significant dissipation at 1048 K (775 °C) is well captured. At the lower temperatures, where a significant dissipation is observed, the dissipation is relatively constant after passing through a maximum at short times and this is the reason for the apparently parabolic experimental kinetics.

To illustrate more clearly the effect of the dissipation from the interaction between the alloying element and the migrating interface, the evolution of the interfacial carbon and Si compositions, as a function of boundary velocity, have been plotted for the alloy containing 0.84 wt pct Si at both 1048 K (775 °C) (Figure 11(a)) and 1123 K (850 °C) (Figure 11(b)). These conditions correspond to the ferrite growth data and calculated free energy dissipations plotted in Figure 7(a) [1048 K (775 °C)] and (d) [1123 K (850 °C)].

Since we consider non-partitioning reactions, the Si content inherited by the ferrite is constant at the bulk value for all boundary velocities. At high boundary velocities, the conditions are very close to PE and the interfacial C contents can be well approximated by the PE model. However, as the boundary velocity decreases the interfacial Si content in the austenite decreases (a negative spike develops). This begins to occur at a boundary velocity of ~1 μm/s at 1048 K (775 °C) and at ~10 μm/s at 1123 K (850 °C). However, in both cases the interfacial C contents are decreasing from the PE

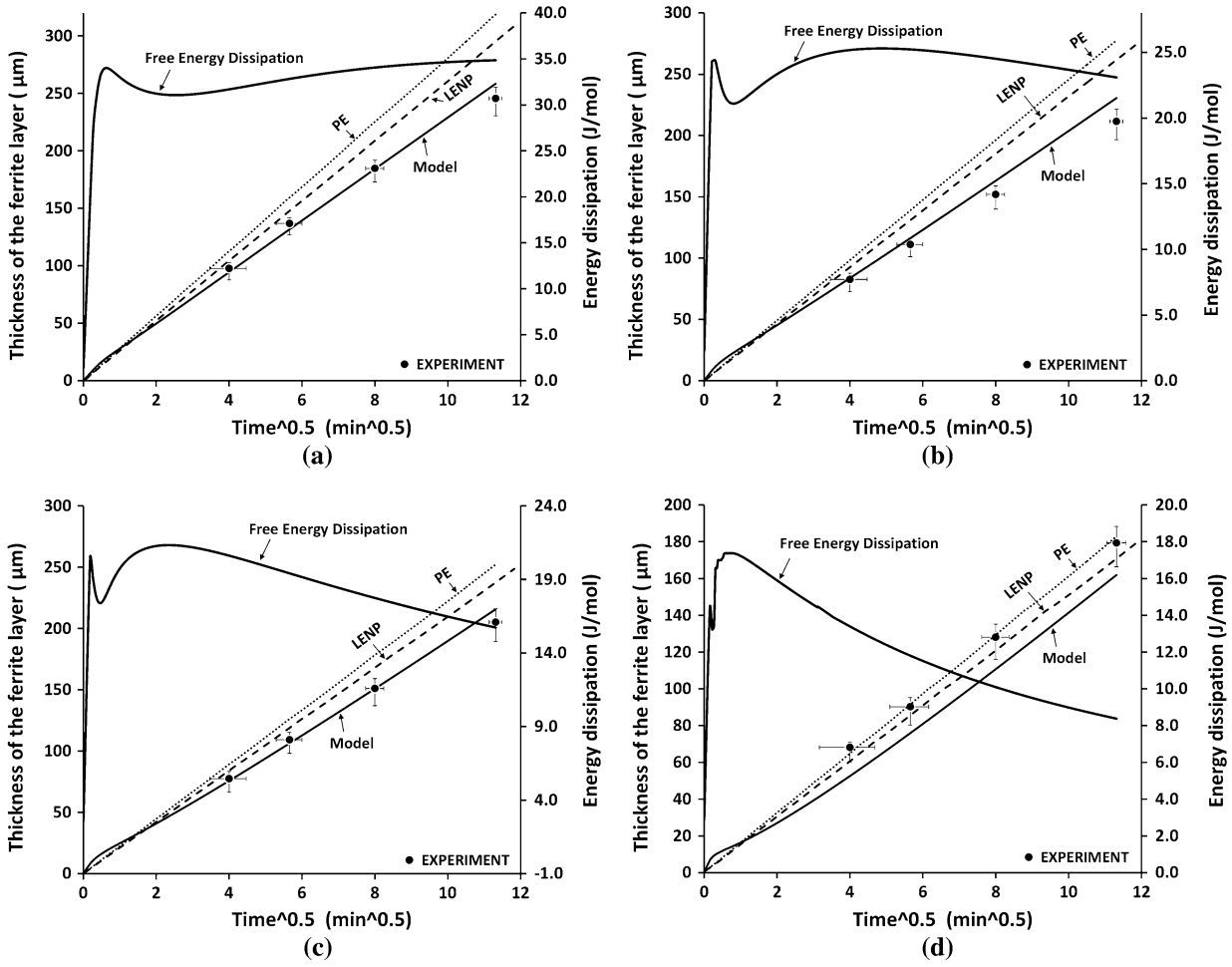

Fig. 10—Experimental ferrite layer growth kinetics measurements from the Fe-0.58C-2.00Cr alloy examined by Beche *et al.*[21]: (*a*) 775 °C, (*b*) 806 °C, (*c*) 825 °C, (*d*) 850 °C. Comparisons with the PE, LENP and Zurob *et al.* model are shown in each case as well as the free energy dissipated during the reaction.

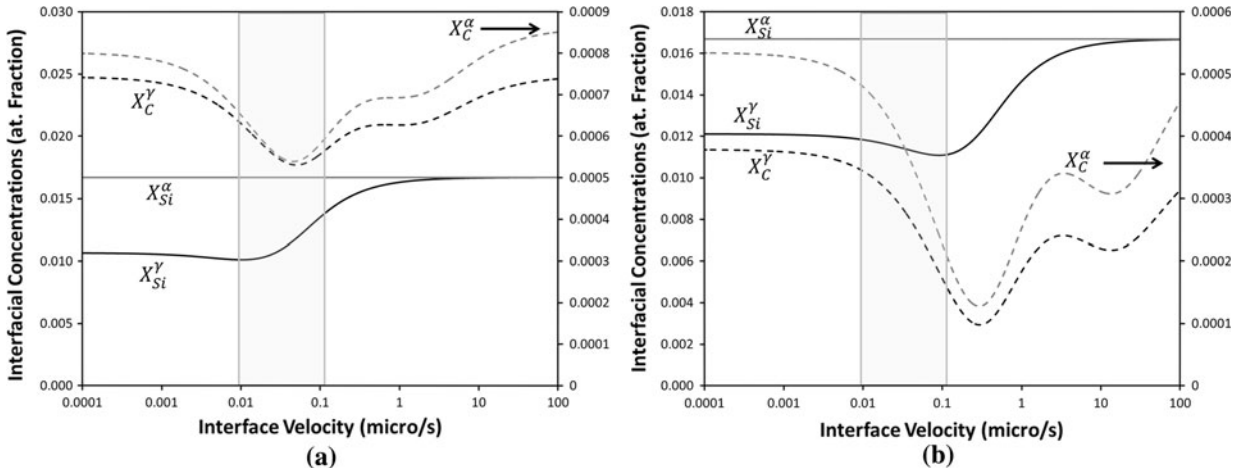

Fig. 11—Evolution of the interfacial contact conditions for C and Si, as a function of boundary velocity for the alloy containing 0.84Si at (*a*) 775 °C and (*b*) 850 °C. The interfacial C content in the ferrite is plotted on the right-hand y-axis. The shaded velocity range (~0.01 to 0.1 mm/s) corresponds the velocity range samples during most of the growth data collected in the decarburization experiments reported in Fig. 7.

values before the negative Si spike starts to develop. This variation in the interfacial contact conditions for C is due to the effect of the dissipation arising from the interaction between the Si and the boundary itself. As the spike develops, which is predicted to occur in this system because of the fast diffusion of Si in austenite at

these temperatures, a further fall in the interfacial C contents is observed. At 1048 K (775 °C) (Fig. 11(a)) the negative Si spike is developing during the velocity regime sampled by the decarburization experiments whereas at 1123 K (850 °C) it is expected that the spike will have already developed very early in the reaction and most of the ferrite growth will occur with a negative Si spike in the austenite (Figure 11(b)). However, once the Si spike is relatively well developed [at v~0.01 μm/s at 1048 K (775°C) and 0.1 μm/s at 1123 K (850°C)] further decreases in the boundary velocity lead to an increase in the interfacial C contents. This increase is due to the decreasing magnitude of the dissipation from the interaction between Si and the boundary (as shown in Figure 7(a) and (d)). This dissipation is close to zero by the time the velocity has fallen to 0.00001 μm/s and the contact conditions for C are then close to the LENP values. During the boundary velocity regime sampled by the decarburization experiments, the interfacial C contents are influenced by both the Si spike and the dissipation associated with the Si interaction with the boundary and both must be considered in this system to reproduce the experimental results. As illustrated by Zurob *et al*. in the companion paper, other alloying elements that may diffuse more slowly than Si in the austenite may offer less of a role for the alloying element spike and it may be the dissipation that dominates effects on the interfacial C contents.

V. CONCLUSIONS

Existing 'solute drag' or 'diffusional dissipation of Gibbs free energy' models suggest both a concentration and temperature dependence, in addition to the well know boundary velocity dependence. The new model for ferrite growth in Fe-C-X systems under non-partitioning conditions proposed by Zurob *et al*.[18] in the companion paper in this volume, captures the effect of solute diffusion across the migrating ferrite/austenite interface using Hillert's diffusional dissipation theory and a rigorous test should include a test of the concentration and temperature dependence. In this contribution, this model has been tested using controlled decarburization experiments. The concentration dependence was tested using six Fe-C-Co alloys ranging from 0.5Co to 20Co, and three Si alloys containing up to 1.5Si. The temperature dependence of the model was tested in an alloy containing 5Co, in all three Si containing alloys and in an alloy containing 2Cr. In all cases, very good agreement with the experimental kinetics was obtained using reasonable choices for the unknown interface thermodynamics and trans-interface diffusivities. This agreement suggests that, over the temperature and compositions regimes studied, these dependencies are well captured by the new ferrite growth model of Zurob *et al*.

ACKNOWLEDGMENTS

CQ acknowledges the award of a Monash Graduate Scholarship (MGS) and an International Postgraduate Research Scholarship (IPRS). HSZ, DP and GP gratefully acknowledge the financial support of the Natural Science and Engineering Research Council of Canada. CRH gratefully acknowledges the award of a Future Fellowship from the Australian Research Council. The authors also wish to acknowledge many stimulating discussions with the ALEMI community.

REFERENCES

1. K. Lucke and K. Detert: *Acta Metall*., 1957, vol. 5, p. 628.
2. J.W. Cahn: *Acta Metall*., 1962, vol. 10, p. 789.
3. K. Lucke and H.P. Stuwe: *Recovery and Recrystallization of Metals*, Himmel, ed., Wiley, New York, 1963, pp. 171–210.
4. K. Lucke and H.P. Stuwe: *Acta Metall*., 1971, vol. 19, p. 1087.
5. C.W. Sinclair, C.R. Hutchinson, and Y. Brechet: *Metall. Mater. Trans. A*, 2007, vol. 38A, p. 821.
6. M. Hillert: *The Role of Interfaces in Phase Transformations. Mechanism of Phase Transformations in Solids*, vol. 33, The Institute of Metals, 1968, p. 231.
7. M. Hillert and B. Sundman: *Acta Metall*., 1977, vol. 25, p. 11.
8. M. Hillert and B. Sundman: *Acta Metall*., 1976, vol. 24, p. 731.
9. G.R. Purdy and Y.J.M. Brechet: *Acta Metall. Mater*., 1995, vol. 43, p. 3763.
10. M. Enomoto: *Acta Mater*., 1999, vol. 47, p. 3533.
11. M. Hillert: *Acta Mater*., 2004, vol. 52, p. 5289.
12. J.R. Bradley and H.I. Aaronson: *Metall. Trans. A*, 1981, vol. 12, p. 1729.
13. K.M. Wu, M. Kagayama, and M. Enomoto: *Mater. Sci. Eng. A*, 2003, vol. 343, p. 143.
14. J. Svoboda, F.D. Fisher, and E. Gamsjager: *Acta Mater*., 2002, vol. 50, p. 967.
15. J. Svoboda, E. Gamsjager, F.D. Fisher, Y. Liu, and E. Kozeschnik: *Acta Mater*., 2011, vol. 59, p. 4775.
16. J. Svoboda and E. Gamsjager: *Int. J. Mater. Res*., 2011, vol. 102, p. 666.
17. J. Odqvist, M. Hillert, and J. Agren: *Acta Mater*., 2002, vol. 50, p. 3211.
18. H.S. Zurob, D. Panahi, C.R. Hutchinson, Y. Brechet, and G.R. Purdy: *Metall. Mater. Trans. A*, 2012, . doi:10.1007/s11661-012-1479-8.
19. A. Phillion, H.S. Zurob, C.R. Hutchinson, H. Guo, D.V. Malakhov, J. Nakano, and G.R. Purdy: *Metall. Mater. Trans. A*, 2004, vol. 35A, p. 1237.
20. C.R. Hutchinson, H.S. Zurob, and Y. Brechet: *Metall. Mater. Trans. A*, 2006, vol. 37A, p. 1711.
21. A. Beche, H.S. Zurob, and C.R. Hutchinson: *Metall. Mater. Trans. A*, 2007, vol. 38A, p. 2950.
22. H.S. Zurob, C.R. Hutchinson, A. Beche, G.R. Purdy, and Y.J.M. Brechet: *Acta Mater*., 2008, vol. 56, p. 2203.
23. H.S. Zurob, C.R. Hutchinson, Y. Brechet, H. Seyedrezai, and G.R. Purdy: *Acta Mater*., 2009, vol. 57, p. 2781.
24. C.R. Hutchinson, A. Fuchsmann, and Y. Brechet: *Metall. Mater. Trans. A*, 2004, vol. 35A, p. 1211.